AIMS Materials Science, 8(2): 301–320.
DOI: 10.3934/matersci.2021020
Received: 22 February 2021
Accepted: 11 May 2021
Published: 14 May 2021

http://www.aimspress.com/journal/Materials

Research article

Influence of fly ash on hydration compounds of high-volume fly ash concrete

M. Kanta Rao[1,2,*] and Ch. N. Satish Kumar[3]

[1] Department of Civil Engineering, Acharya Nagarjuna University, Guntur, Andhra Pradesh 522510, India
[2] Department of Civil Engineering, V.R. Sidhartha Engineering College, Vijayawada, Andhra Pradesh, 520007, India
[3] Department of Civil Engineering, Bapatla Engineering College, Bapatla, Andhra Pradesh, 522102, India

* **Correspondence:** Email: mkrao99ce@vrsiddhartha.ac.in; Tel: +919848316175.

Abstract: Development of sustainable materials has become one common goal across the globe to meet the ever-increasing demand for the construction materials. High volume fly ash (HVFA) concrete is one such sustainable construction material which utilizes fly ash in concrete as a partial replacement of cement. Though the existing literature focuses abundantly on high volume fly ash concrete, the present work aimed to explore the intricate hydration process thorough a systematic experimental program. A series of experiments including compressive strength, rapid chloride permeability, UPV, acid resistance, X-ray diffraction, SEM and EDAX were performed to examine the effect of varying proportions of fly ash (0%, 20%, 40%, 60%) on cement replacement. Analysis of results indicated formation of hydration compounds in the form of alite, belite, celite, portlandite and tobermorite (C-S-H gel). Results of mechanical and durability tests showed that, to achieve maximum benefits, cement can be replaced to an optimum value of fly ash of 40%. The authors believe that the formation of hydration compounds tobermorite and celite resulted in attaining enhanced durability and strength in high volume fly ash concrete.

Keywords: HVFA concrete; compressive strength; RCPT; UPV; acid resistance; X-ray diffraction (XRD) and energy dispersion spectroscopy; scanning electron microscopy

1. Introduction

The production of cement involves in several stages of manufacturing process and utilizes greenhouse gases. It was predicted that the demand for cement may be beyond 6 Giga tones (Gt/year) by 2050 [1]. The production of 1-ton cement leads to release of one-ton carbon dioxide in the atmosphere [2]. The energy consumption involved in cement production leads to approximately 7% of worldwide CO_2 emission. Carbon dioxide is responsible for global warming and it occupies a major part of greenhouse effect [3]. Thermal power plants are major source of fly ash which is the by-product of pulverized coal. It is collected by electrostatic precipitators in the thermal power plants. Fly ash is a pozzolanic material which comprises of SiO_2, Al_2O_3, Fe_2O_3 compounds which present in amorphous form. This amorphic structure results in pozzolanic activity to fly ash. When fly ash with oxides of aluminum, silica and iron react with calcium based OPC then portlandite, tobermorite and calcium aluminum hydrates were formed [4]. Later the researchers investigated advantages contributed by use of sound quality fly ash in concrete like enhanced workability, strength improvement, impermeability, and durability at later stages, reduction in heat of hydration and reduction of drying shrinkage [5]. Furthermore, utilization of fly ash resulted in reducing drying shrinkage, resistance to acid attack and deterioration thus reducing the possibility of corrosion of rebar [6]. Replacement of fly ash with the binder resulted in decrease of porosity of concrete by filling the voids between aggregates continuously [7]. The chloride permeability of concrete can be effectively reduced by replacing fly ash as fineness which involve in the minimization of chloride permeability [8]. In order to utilize the supplementary cementitious materials like fly ash in high volumes, keen understanding of complex processes which occur during hydration process is vital [9]. Accurate investigation of volume fraction of phases in the cement composite system involves in the determination of degree of hydration of cement and fly ash systems. Experimental methods used in order to determine the degree of hydration are heat of hydration method, portlandite measurement method and XRD analysis method [10]. Addition of fly ash in concrete reduces the drying shrinkage resulting in the formation of fewer cracks. Thus, resistance to deterioration can be achieved [11]. The concrete mixture comprises of combined micro-structure which causes difficulty to study its micro-structure due to the presence of high-level heterogeneity. This difficulty can be overcome with the use of XRD technique. The quantitative analysis of crystal structure of mineral compounds which form microstructure of concrete can be categorized effectively [12]. The parameters such as crystallinity, particle size distribution, morphology is influencing the hydration mechanism which resulted in variation of mechanical and durability properties of concrete [13]. By reviewing hydration mechanism of high-volume fly ash concrete (HVFA), it was observed that the strength gain is not solely depending on C-S-H gel formation. Other hydration products like carbo-aluminates also found to be the contributors of gaining strength of concrete [14]. Using supplementary cementitious materials like fly ash and rice husk ash in the proportion of equal weight resulted in attaining more strength and resistance to chloride ion permeability [15]. In the cubes cast with lime fly ash composites, tobermorite and calcite were the main contributors of strength [16]. The experimental investigations revealed that the degradation of specimen, erosion and spalling were main products of acid-cement reaction products which resulted in the weight reduction and deformations occurred in the specimens [17]. The grain size of fly ash influences its role of filling. Smaller size particles fill the voids between cement particles and reduce the filling of water [18]. Resistance to acid attack of HVFA cement pastes and mortars was sufficient resulting in the severe disintegration of samples [19].

Using HVFA (>70%) with activated blends of OPC resulted mainly in the C-S-H gel and N-A-S-H formation [20]. Fly ash acts as micro aggregate. With the increase in fly ash content, micro aggregate action will be strengthened and weakens with age [21]. Addition of fly ash leads to the stabilization of ettringite conversion to mono sulphate due to the presence of alumina in excessive amounts compared to OPC [22]. The slow pozzolanic reaction was due to the presence of zeolite in the mix with high dosage of fly ash content at later ages of hydration [23]. Fiber reinforced concrete with high volume fly ash attained strength twice to the strength attained by the concrete without fly ash [24]. From the experimental results, it was concluded that fly ash can be replaced up to 50% and the blended concrete can be used in reinforced concrete structures and precast elements [25]. The aforementioned literature indicates that HVFA concrete have the potential in terms of durability as well as strength. In addition to that, it will effectively reduce the emission of CO_2 due to the reduced usage of cement content in concrete.

Though the mechanical properties were significant to evaluate the performance of fly ash replacement in concrete in excess amounts, there is still scope to assess the hydration mechanism through micro level studies. In light of this, the current study assesses the hydration process in connection with mechanical characteristics through a systematic investigation.

2. Materials and methods

2.1. Materials

The materials used in testing were ordinary Portland cement (OPC) corresponding to 53 grade and fly ash of class F. The source of fly ash was Narla Tata Rao Vijayawada Thermal Power Plant. Table 1 demonstrates the chemical composition of ordinary Portland cement and fly-ash. The specific gravity of fly ash is 2.3 and fly ash % that was retained on 90 μm sieve is 10. Properties of OPC were given in Table 2. The coarse aggregate with combinations of 20 mm, 12 mm sizes and fine aggregate were used in the mix. The physical properties of fine and coarse aggregates were given in Table 3. The concrete mix with 400 kg/m^3 binder content with 0.45 water-binder ratio (w/b) and fly ash with the varying proportions of 0%, 10%, 20%, 30%, 40%, 50%, and 60% were used in the preparation of specimens. The mix proportions of different concrete mixes were calculated by using Abraham's law which are tabulated in Table 4.

Table 1. Chemical composition of OPC and fly ash.

Compound	Percentage present in OPC	Percentage present in fly ash
CaO	63.7	0.768
SiO_2	18.94	60.76
Al_2O_3	4.72	30.96
Fe_2O_3	4.24	3.51
MgO	2.21	0.79
K_2O	0.53	1.12
SO_3	2.19	-
Na_2O	0.62	-
P_2O_5	-	0.164
Loss of ignition	2.85	1.9

Table 2. Properties of OPC.

Physical property	OPC
Fineness (%)	8.0
Specific surface (cm^2/g)	3503
Normal consistency (%)	29
Initial setting time (min)	50
Final setting time (min)	210
Compressive strength at 7 days (MPa)	39
Compressive strength at 28 days (MPa)	56.8
Relative density	3.13
Soundness(mm)	1.2

Table 3. Physical properties of fine aggregate and coarse aggregates.

Physical property	Fine aggregates	Coarse aggregates
Relative density	2.67	2.71
Fineness modulus	2.35	6.4
Unit weight (kg/m^3)	1700	1650

Table 4. Mix proportions of fly ash blended cement concrete.

Mix	% replacement of cement by fly ash	Cement (kg/m^3)	Fly ash (kg/m^3)	Water (kg/m^3)	Water-binder ratio	Fine aggregate (kg/m^3)	Coarse aggregate (kg/m^3)
C1W1F0	0	400	0	180	0.45	737.6	1106.4
C1W1F1	10	360	40	180	0.45	731.7	1097.56
C1W1F2	20	320	80	180	0.45	725.79	1088.7
C1W1F3	30	280	120	180	0.45	719.86	1079.8
C1W1F4	40	240	160	180	0.45	713.95	1070.9
C1W1F5	50	200	200	180	0.45	708	1062
C1W1F6	60	160	240	180	0.45	702.1	1053

C1: binder content; W1: water binder ratio; F0: 0% fly ash; F1: 10% fly ash.

Based on the Bougee's equations to determine the hydration compounds were assessed from chemicals which were disclosed after the chemical analysis of the Portland cement. From the theoretical analysis, it was found that the presence of alite (C_3S) was 68% which is responsible for early strength and belite (C_2S) was 17% responsible for long term strength in the concrete, celite (C_3A) was about 9% which reduce the chance of vulnerability at acid ingressive environments and felite (C_4AF) about 7% which retards the vigorous reaction and formation of crystals.

2.2. Tests performed

2.2.1 Compressive strength test

The compressive strength of concrete is a unit to assess the performance of concrete in order to satisfy the strength and durability requirements. It is termed as the resistance to failure under the action of compressive force. The cubes of 100 mm size after 7, 28 and 56 days were tested for compressive strength on compression testing machine of 3000 kN capacity according to the specifications corresponding to the [26]. The compressive strength was calculated by dividing the failure load with area of application of load.

2.2.2 Rapid chloride permeability test

The resistance to chloride ion permeability of fly ash concrete was determined as per the specifications confirming to ASTM (1202) [27]. This test includes the determination of the electric conductance for different grades of concrete mixes and the rapid indication of its resistance to pass the ions through the specimen of 100 mm diameter and 50 mm height. It involves in the process of monitoring amount of electric current passed through the specimen over a specified time. It is a measure of assessing the impermeability of concrete to pass the chloride ions through it. The specimen was clamped in between the test cell. The cell which was connected to negative terminal of power supply was filled with 3% NaCl solution and the cell connected to the positive terminal was filled with 0.3 M NaOH solution. The boundary of specimen and cell were sealed with the help of sealant. After connecting the cables to the cell, access the power supply with 60 V. The test setup was shown in Figure 1.

Figure 1. Rapid Chloride Permeability Test set-up.

2.2.3 Pulse velocity test

Ultrasonic pulse waves were transmitted through the specimen and the time taken by the wave to transmit through the specimen was measured as per BIS 13311-92 Part 1. The pulse velocity is the ratio of width of specimen and the time of travel by the pulse in it. In this test, the waves were

transmitted through the 150 × 150 mm specimens of 7, 28 and 56 days respectively. The criteria for assessing concrete quality were tabulated in the Table 5 and test set up was shown in the Figure 2.

Table 5. Grading concrete quality as per BIS 13311-92 Part 1.

Pulse velocity (km/s)	Concrete quality grading
Above 4.5	Excellent
3.5 to 4.5	Good
3.0 to 3.5	Medium
Below 3.5	Doubtful

Figure 2. UPV test setup.

2.2.4 Acid attack test

The resistance offered by the concrete specimen when it was subjected to acidic atmosphere was determined by performing this test as per ASTM C 267 (2012). It is a tool of assessing the durability of concrete without any deterioration. In this test, the test specimens after their corresponding curing ages were immersed in sulphuric acid solution with the concentrations being 1%, 3%, 5% by volume of water. The specimens were under monitoring and pH value of solution was maintained thoroughly. For every 7, 28, 56 days immersion period, the cubes were tested for compressive strength and aesthetics were checked. The loss of strength determines the deterioration rate and the impact of acid attack on specimen surface.

2.2.5 X-Ray diffraction test

X-ray diffraction based on quantitative phase analysis is a prevalent technique used to study the hydration of cementitious systems. The specimens which were subjected to compressive strength resulted in crushed powder. The powdered sample for the respective fly ash proportions were sieved through a 90 μm sieve were collected for testing include samples obtained from 0%, 20%, 40%, and 60% fly ash proportions at hydration days of 7, 28, 56 days. Hydrated cement often comprises of several amorphous or nano-crystalline phases. The mineralogical composition of binder and the reactions during hydration of cement attribute a vital role in the determination of phase transformation and mechanical properties of the concrete. The target utilized in X-ray tube was

copper (Cu) with the voltage of 40 kV and 15 mA current. The sample was scanned at a haul of 2θ with the range of scan being 0° to 80°

2.2.6 Scanning electron microscopy

Scanning electron microscopy (SEM) works on the principle of scattering effect. When a beam of electrons passed on to the specimen, the primary electrons get dissipated and some of them would be back scattered. The electrons that were dissipated in the specimen tend to form an interaction front which is vulnerable to the resolution of image formed for each signal. The inclining voltage and atomic number of the sample determines typical depth and shape of the interaction front.

2.2.7 Energy dispersion spectroscopy

The EDS analysis involves in confirmation of firmness of microstructure study conducted on concrete samples. It is a standard technique used to study the chemicals present in the sample at micro level. It reveals the existence as well as relative abundance of elements in the sample. This test can be performed along with the XRD analysis or SEM. The count of X-ray and its corresponding energy was measured in an X-ray detector. Energy of the X-ray is the distinctive of chemical element from which X-ray was scattered.

The area on which electron beam was being excited in order to determine the energy of X-ray discharged was determined. The quantitative analysis involves in the estimation of relative existence of elements by peak intensity. As every element has its atomic configuration, unique set of peaks were used to identify a particular element in the sample. In this analysis, the weight percentage of various mineral elements present in the sample was classified. With the help of mass percentage, the characteristics of each sample can be obtained.

3. Results and discussion

3.1. Compressive strength

The compressive strength test was performed for the specimens of size 100 × 100 × 100 mm with varying fly ash content and control sample at 7, 28, 56 days and results were plotted in Figure 3. From the graph, it was observed that the compressive strength was maximum for control specimen at 7 days. The early strength was majorly influenced by the physical presence of ash particles rather than the pozzolanic reaction. At the hydration age of 28 days, the higher compressive strength was spotted at 30% fly ash content because of the pozzolanic reaction and the presence of belite (C_2S) in higher quantity. Even though the compressive strength obtained at 30% fly ash content has higher value and compressive strength related to 40% fly ash content resulting in higher value compared to the control sample due to the presence of oxides of silica and alumina which contributes strength and durability of concrete. At 56 days, even though compressive strength related to 40% fly ash content is higher than the control sample. This includes that the utilizing high volume of fly ash also resulting in the higher strength attainment compared to the control mix.

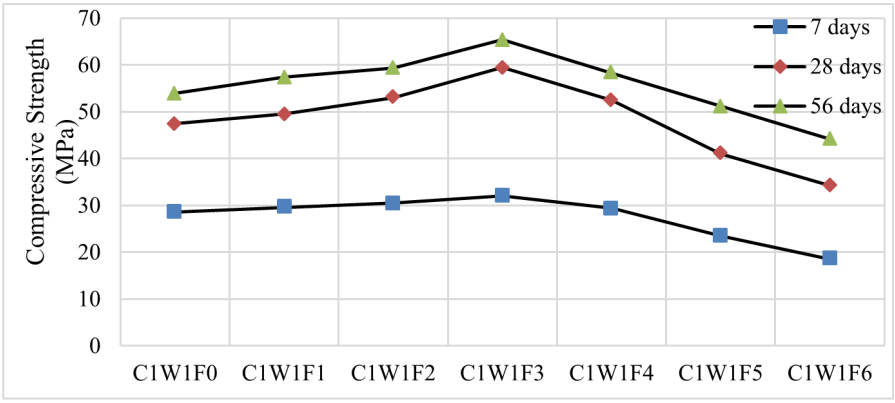

Figure 3. Compressive strength of specimens.

3.2. Rapid chloride permeability test

The rapid chloride permeability test (RCPT) values for the specimens with various fly ash replacements at a w/b ratio of 0.45 were plotted in Figure 4. From the graph, it was observed that the charge passed through control sample was more compared to specimens with varying proportions of fly ash content. The RCPT values were decreasing with increase in fly ash content. From the micro structural analysis, it was observed that the hydroxyl ions present in the pore solution were bounded by the fly ash particles which resulted in the reduction of alkalinity of pore solution. Thus, dissolution of aggregate was minimized leading to extenuation of alkali silica ratio through which low chloride permeability was observed in the specimens with fly ash content compared to control specimen.

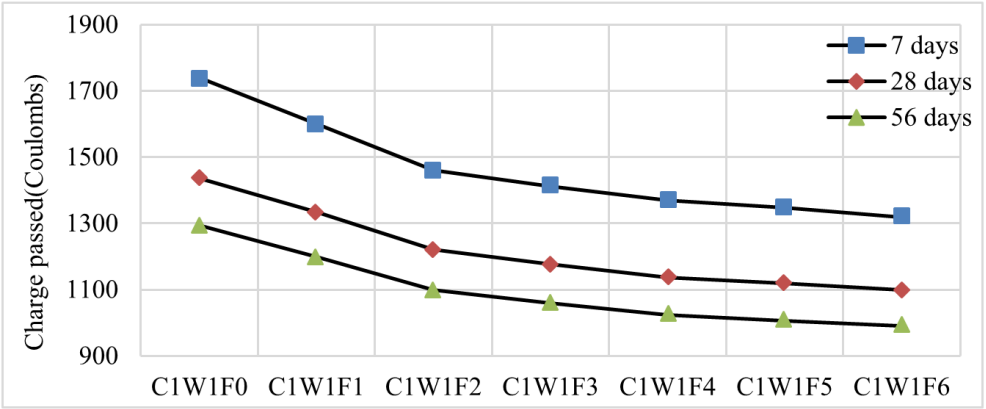

Figure 4. Rapid chloride permeability test results for binder content of 400 kg/m^3 at W/B ratio of 0.45.

3.3. UPV test

The pulse velocity of the waves transmitted through the specimens at 7, 28 and 56 days was tested. The variation of pulse velocity values was shown in Figure 5. The velocity of the specimen

with blended fly ash resulted in higher values compared to the control specimen up to the 30% fly ash replacement at 28, 56 days respectively. The increase in velocity was due to the gradual pozzolanic reaction which tends to bind the particles by avoiding voids. This resulted in the higher UPV results for all the fly ash replacement proportions when compared to the 7 days results.

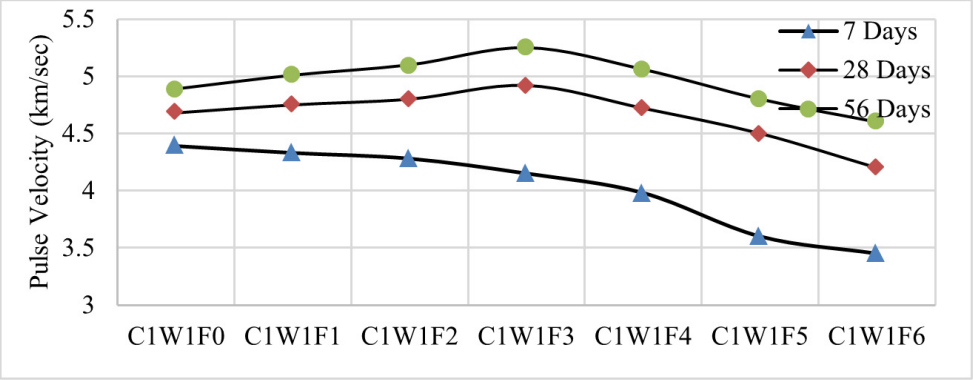

Figure 5. UPV test results.

3.4. Acid attack

The loss percentage of compressive strength for the specimens with cement content of 400 kg/m^3 with water-binder ratio of 0.45 when immersed in H_2SO_4 solution at 7 days were plotted in Figure 6. The loss percentage of strength was majorly observed for the spceimens immersed in 5% H_2SO_4 solution. Highly soluble salts of calcium was precipitated when the portlandite and sulfuric acid react with each leading to the degradation of concrete. The control sample was majorly affected by the acidic solution compared to the specimens with fly ash content for all concentrations of acid. The percentage loss of strength for control sample when immersed in H_2SO_4 solution for 7 days was 26.37% which was reduced to 12.77% for the specimen with 60% fly ash content.

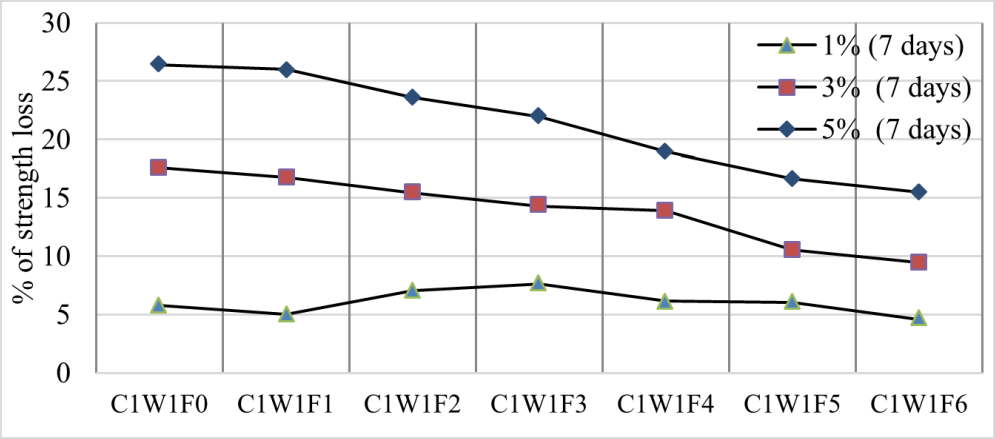

Figure 6. Percentage of strength loss when specimens were immersed in H_2SO_4 solution at 7 days.

The speciemens with cement content being 400 kg/m^3 with water-binder ratio of 0.45 were immersed in H_2SO_4 solution at an immersion period of 28 days. The percentage of strength loss was plotted in Figure 7 respectively. It was observed that the percentage of strength loss was less for the specimens immersed in 1% H_2SO_4solution because the deterioration is proportional to concentration of acid solution. For 5% concentration, the percentage loss of strength was 39.5 which was decreased to 23.51 for the specimen with 60% fly ash content.

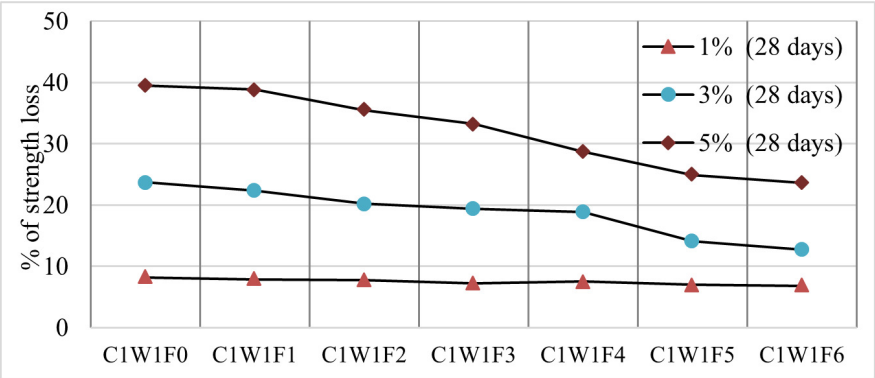

Figure 7. Percentage of strength loss when specimens were immersed in H_2SO_4 solution at 28 days.

The percentage of strength loss was 49.38% for the control sample immersed in 5% H_2SO_4 solution which was decreased to 29.51% with the replacement of 60% fly ash content in the Figure 8. From the graphs and results obtained above, it was noticed that with the increase in fly ash content the impact of sulfate attack was being decreased for all the proportions of fly ash and hydration days. The control sample was vulnerable to the sulphate attack because of the absence of celite compound. The samples which were immersed in 5% H_2SO_4 solution with variying proportions of fly ash content were less vulnerable compared to the control sample. With the addition of fly ash the sulfate attack on concrete was minimized effectively because of the resistance offered by fly ash to diffuse the particles and by stabilizing calcium aluminium hydrates within the binder.

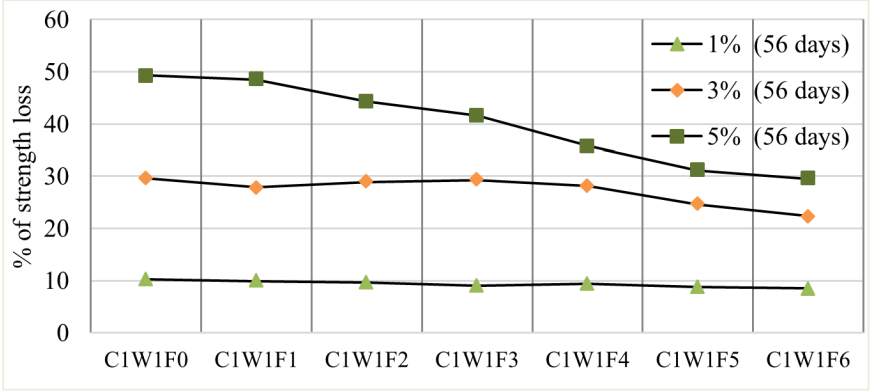

Figure 8. Percentage of strength loss when specimens were immersed in H_2SO_4 solution at 56 days.

The percentageof weight loss of the speciemens when immersed in various concentrations of H_2SO_4 solution at an immersion period of 7 days were plotted in Figure 9 respectively. The percentage of weight loss was majorly observed in the specimens immersed in 5% H_2SO_4 solution. The percentage of weight loss for control sample at 1% H_2SO_4 solution was 0.43 which was decreased gradually to 0.15 upon 60% replacement of fly ash content. It was 2.36 % for the control sample at 5% H_2SO_4 solution which was decreased to 0.62% at 60% flyash content.

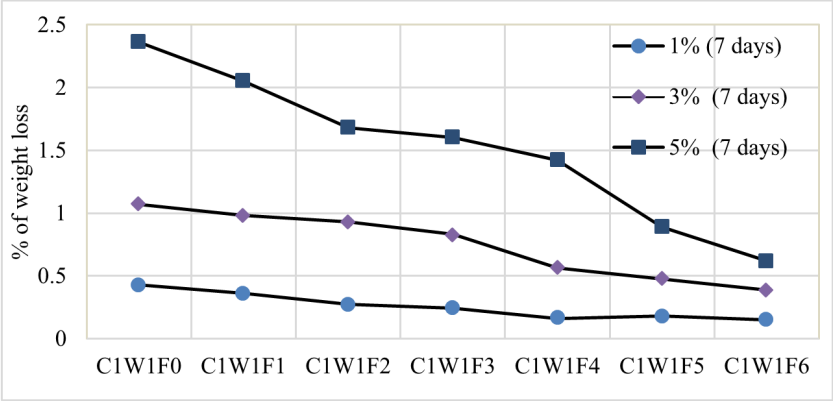

Figure 9. Percentage of weight loss when specimens were immersed in H_2SO_4 solution at 7 days.

The specimens with 0.45 water-binder ratio with 400 kg/m^3 were immersed in various concentrations of sulphuric acid for 28 days were plotted in Figure 10. The percentage of weight loss was majorly spotted for 5% H_2SO_4 solution with 7.1% which gradually decreased to 2.8% at 60% fly ash content. It was 3.8% for control sample at 3% H_2SO_4 solution which reduced to 1.08% upon replacement of 60% fly ash content.

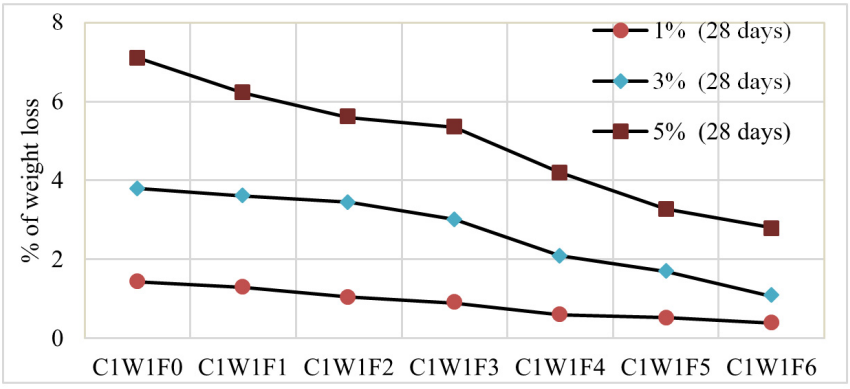

Figure 10. Percentage of weight loss when specimens were immersed in H_2SO_4 solution at 28 days.

The percentage of weight loss when the specimens with 400 kg/m^3 binder content and water-binder ratio being 0.45 when immersed in various concentrations of H_2SO_4 solution at 56 days

were plotted in Figure 11. It was 8.75% for the control sample when immersed in 5% H_2SO_4 solution which gradually decreased to 4.95% for the specimen with 60% fly ash content.From the graphs obtained, it was noticed that the major strength loss was observed for control specimen at all hydration days. The specimens with high volume fly ash replacement resulted in the lower values of strength loss. The loss in weight of specimen was due to sulphate attack. Leaching of calcium sulphate occurs when sulphate ions react with portlandite resulting in the weight loss and deterioration of concrete. From microstructural analysis, it was observed that with the increasing fly ash content the portlandite was decreased which resulted in counteracting the suplhate attack and increased durability of concrete.

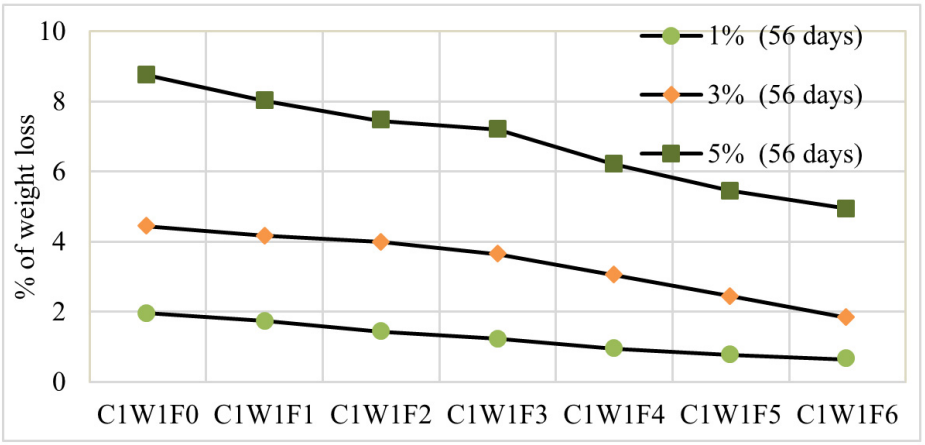

Figure 11. Percentage of weight loss due to immersion of specimens in H_2SO_4 solution at 56 days.

The percentage loss of strength and weight was majorly observed at an immersion age of 56 days. Figure 12 represents the deterioration of the speciemns with binder content of 400 kg/m^3 and water-binder ratio of 0.45 were immersed in H_2SO_4 solution of 5% concentration at an immersion period of 28 and 56 days. Incorporation of fly ash minimized the effect of acid attack by resisting the diffusion of particles. When compared to the control specimen, the speciemns with fly ash was observed with less amount of salt precipitation. It is evident from the Figure 12 that the additon of fly ash resulted in the decreased rate of deterioration relatively.

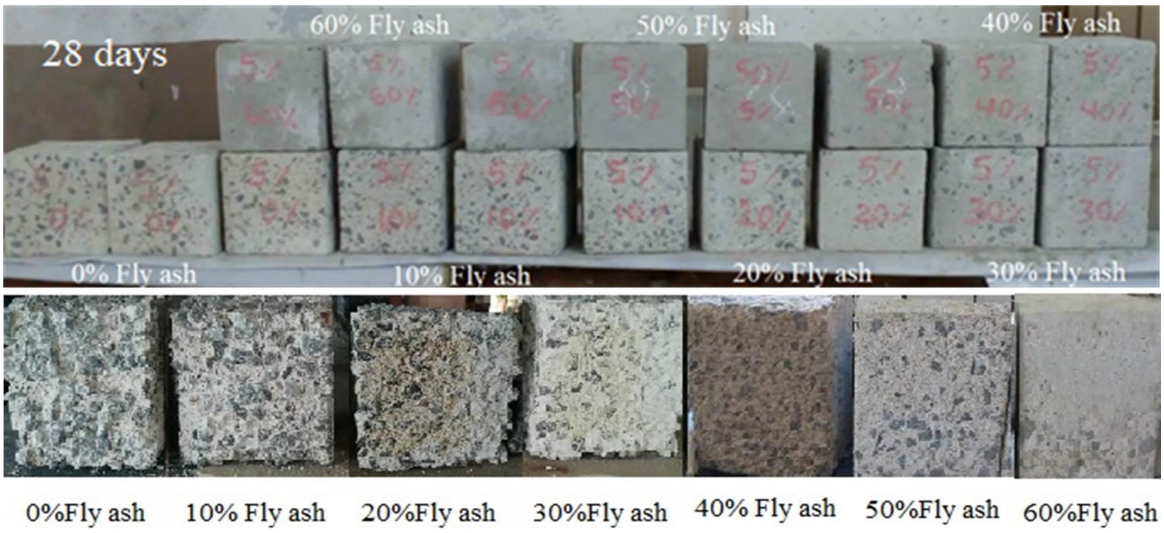

Figure 12. Deteriorated samples after immersing in acid at 28 and 56 days.

3.5. Micro structural analysis

It was observed that due to early stage of hydration process, the formation of portlandite (CH) was rapid because of freely available lime resulting in the higher peak in the 7 day graph of Figure 13. At later stages of hydration, the consumption of freely available portlandite was higher resulting in the decrease of CH peak in 28 days graph. Corresponding decrease in the portlandite formation in 28 days leads to increase in formation of tobermorite (C-S-H) and its hydrated products which are alite (C_3S). belite (C_2S). It was also evident from Figure 14 that due to the formation of needle like crystals (ettringite), the Interfacial transition zone (ITZ) was initiated which resulted in increasing the pore size of the particle. Due to the absence of pozzolanic activity, alite (C_3S) was higher which contributes early strength (7 days) and at 28, 56 days belite (C_2S) was observed which is a contributor of later strength. The early strength of control sample was higher when compared to the other samples with varying proportions of fly ash content because of the presence of alite in higher amounts and reaction of free lime even at curing stage also. From the EDS graph obtained for control sample at various hydration days, it was noticed the peak of calcium was high when compared to the other compounds. Since there is no supplementary cementitious material calcium existed in higher amounts.

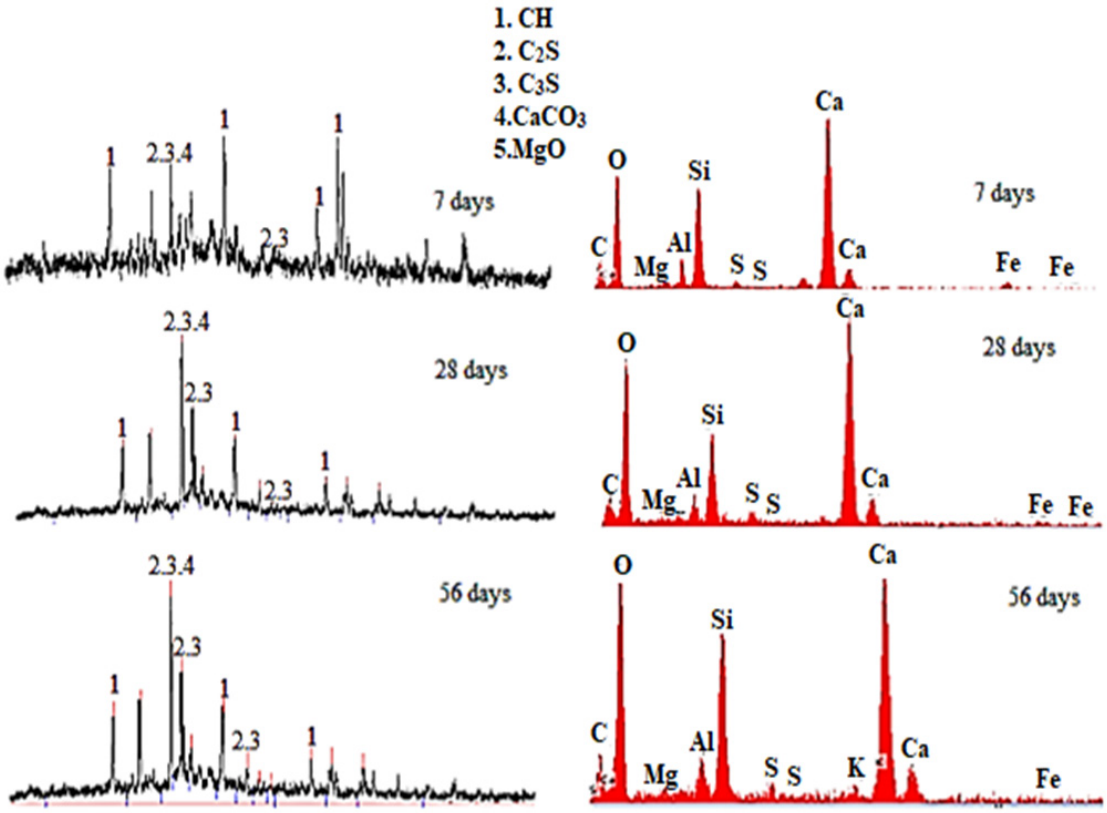

Figure 13. XRD image obtained for sample without fly ash at 7, 28, 56 days and their corresponding EDS graphs.

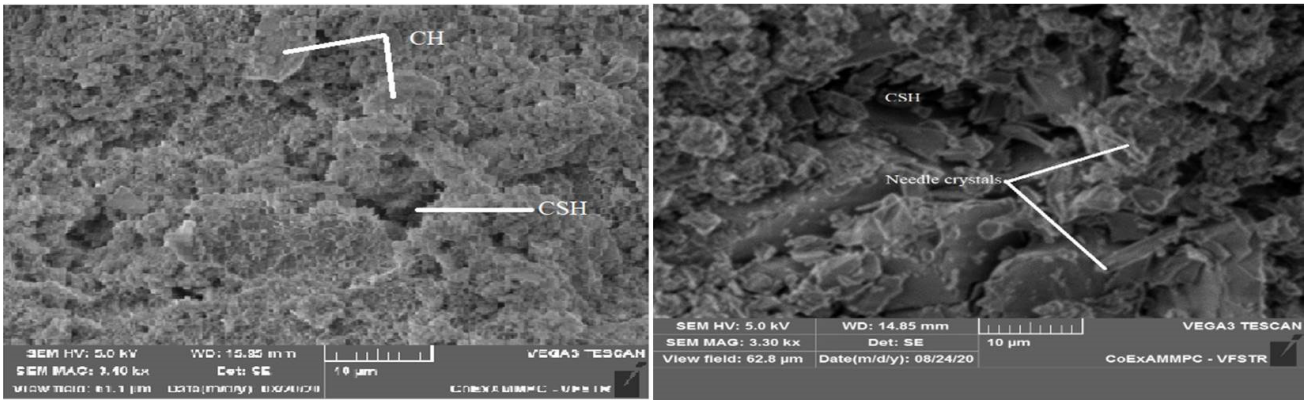

Figure 14. SEM images of sample without fly ash at 56 days.

The constant decrease of portlandite and corresponding increase of tobermorite were observed from the XRD graph at various hydration days was represented in Figure 15. With the visual evidence from the Figure 16 obtained the ettringite which had needle like structure was converted into crystalline tobermorite due to the binding of particles. Due to the constant consumption of CH by the pozzolanic activity there was no amount of portlandite in order to react with the dissolute ions which cause delay in the attainment of compressive strength in early stages. The formation of alite which is a contributor of early strength and belite compound was increased due to the pozzolanic

action. After 28 days, a drastic change in carbonation was observed which attributed to the reaction of $CaCO_3$ with $Ca(OH)_2$ and fly ash resulting in the increase of C-S-H formation along with carbonate compounds. From the EDS graphs obtained for 20% fly ash samples at 7, 28, 56 days it was observed that the quantity of calcium was decreasing compared to the control sample and the hydration ages.

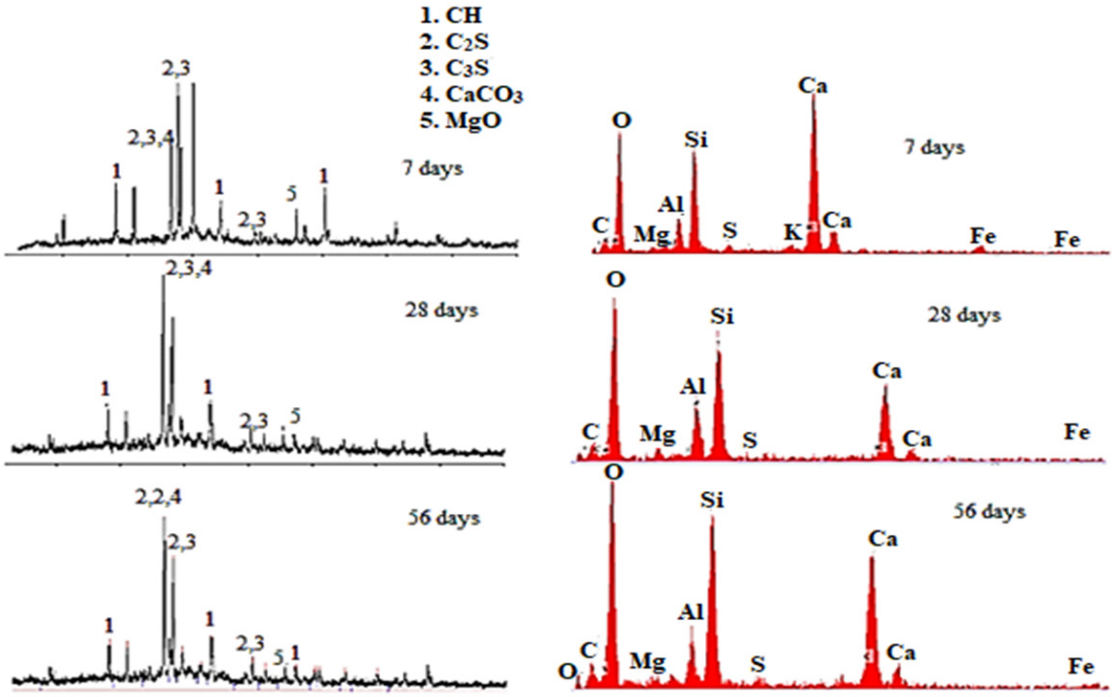

Figure 15. XRD image and corresponding EDS graph obtained for 20% fly ash sample at 7, 28, 56 days.

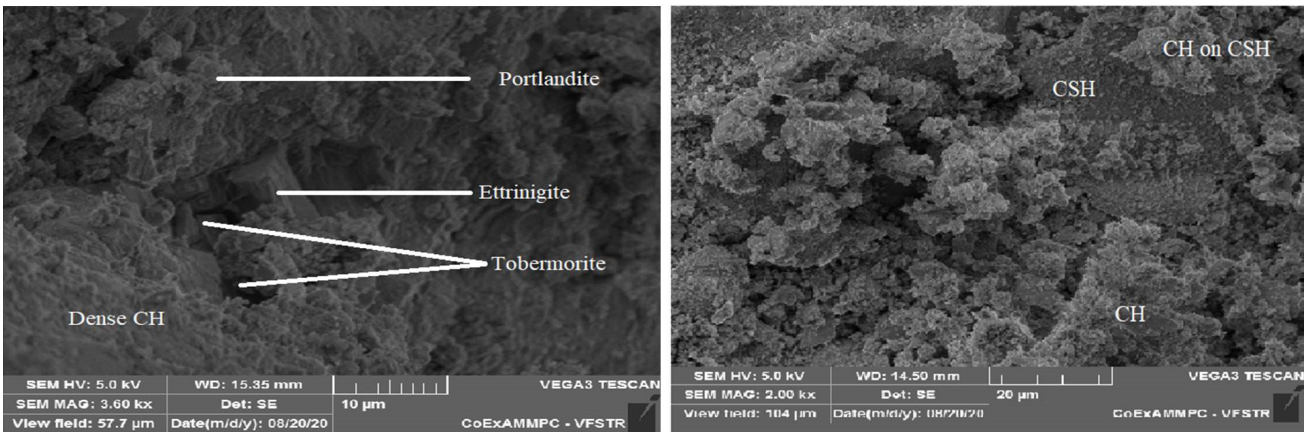

Figure 16. SEM image of sample with 20% fly ash replacement at 56 days.

The silica content was increasing with increase in fly ash content. The oxides of various compounds resulted in the oxide peak. The constant decrease of portlandite gel was spotted with the

increase of fly ash content resulting in the formation of CSH peak and its hydrated products such as magnesium oxide, calcium carbonate along with alite and belite compounds were spotted in Figure 17. Due to the formation of hexagonal crystals, the conversion of ettringite to monosulphate reaction was gradually decreased resulting in the freely available portlandite which was shown in Figure 18. The magnesium oxide helps to promote the hydration reaction of alite and belite. This is the reason for the high strength attainment in the samples with fly ash content around 30%. From the EDS graphs obtained for various hydration days, it was observed that the calcium content was decreased with the corresponding increase in silica content. Since the fly ash contains high amount silicates, the peak of silica was noticed with increase of fly ash content. The calcium content was consumed by the formation of CSH gel due to the pozzolanic reaction.

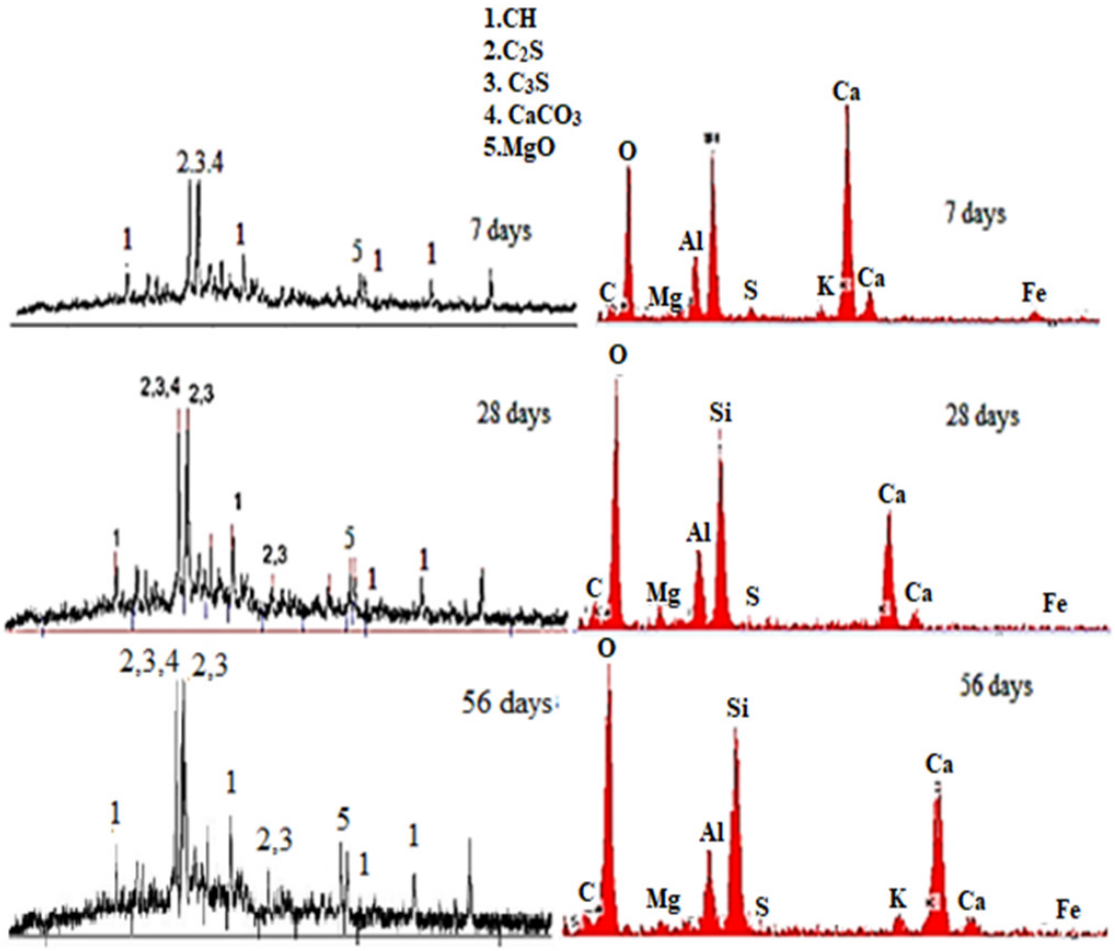

Figure 17. XRD image and corresponding EDS graph obtained for 40% fly ash sample at 7, 28, 56 days.

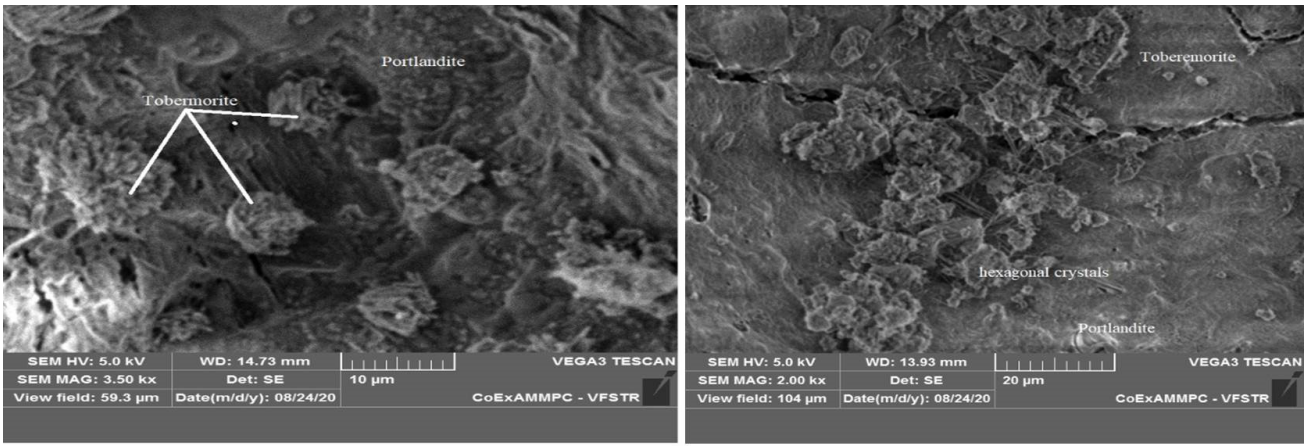

Figure 18. SEM image of sample with 40% fly ash replacement at 56 days.

It was observed that due to the presence of fly ash in high volume, the quantity of portlandite was reduced to minute amounts due to vigorous pozzolanic action in the Figure 19. The quantity of tobermorite (C-S-H) gel was being increased as long as the consumption process of portlandite was continued.

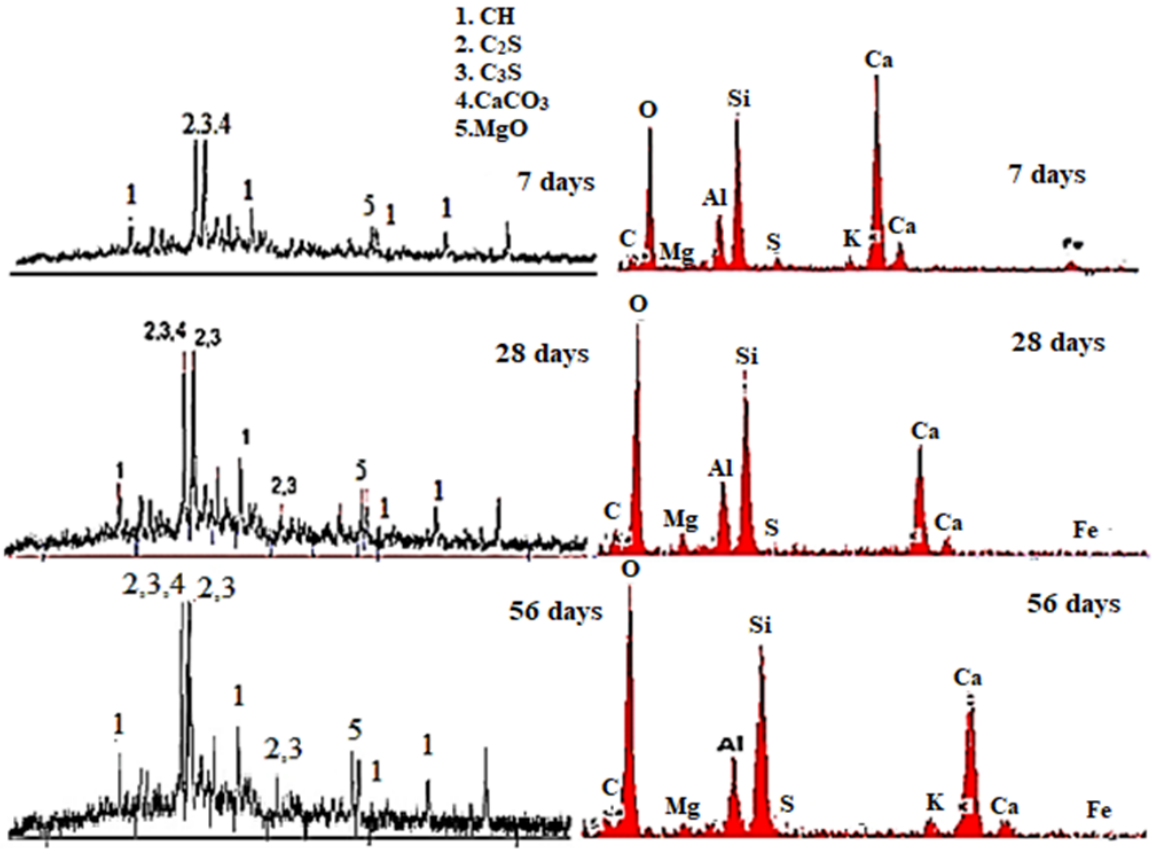

Figure 19. XRD image and corresponding EDS graph obtained for 60% fly ash sample at 7, 28, 56 days.

After the exhaustion of portlandite formation, the quantity of tobermorite was reduced by producing hydration compounds like alite (C_3S), belite (C_2S), MgO and carbonate compounds. Figure 20 represesmts the formation of dense C-S-H crystals.

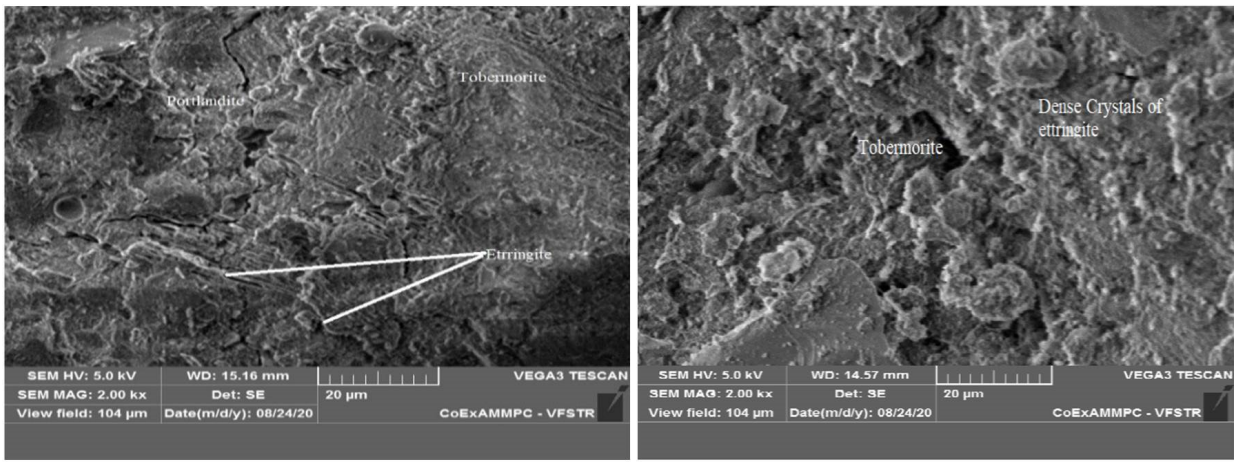

Figure 20. SEM image of sample with 60% fly ash replacement at 56 days.

4. Conclusions

The present study was performed to evaluate the complex hydration and mechanical behavior of HVFA concrete. Based on the experimental results obtained the conclusions were made:

(1) The amorphous silicates in the fly ash react with tobermorite which had crystal structure resulted in the reduction of portlandite as well as increase of CSH gel enhanced the binding capacity by the pozzolanic activity.

(2) The formation of portlandite is harmful for the durability of concrete in terms of acid attack which was reduced with the increase of fly ash content leads to the reduction of capillary pores which result in the decreased diffusion of particles.

(3) Fly ash tends to contribute compressive strength when the aluminosilicates present in the fly ash react effectively with calcium aluminosilicates in cement. Due to this reason the early strength of sample containing fly ash resulted in lesser value when compared to the control specimen. Gradual increase in the compressive strength at later stages was due to the high-volume fly ash and the long term pozzolanic reaction.

(4) Though the fly ash up to 30% reflected maximum strength gain, considering all mechanical as well as durability properties, optimum value of 40% fly ash replacement was proposed considering superior all round performance in comparison to concrete without fly ash replacement at 28 days.

(5) Micro structural analysis revealed that with the addition of fly ash, the density of binder matrix was increased by the pozzolanic reaction. Replacement of fly ash decreased the diffusion of particles and access the equilibrium of CAH hydrates thus increase durability of concrete.

Conflict of Interest

All the authors declare that there is no conflict of interest.

References

1. Kumar M, Sinha AK, Kujur J (2021) Mechanical and durability studies on high-volume fly-ash concrete. *Struct Concr* 22: E1036–E1049.
2. Prakash R, Thenmozhi R, Raman SN, et al. (2020) Characterization of eco-friendly steel fiber-reinforced concrete containing waste coconut shell as coarse aggregates and fly ash as partial cement replacement. *Struct Concr* 21: 437–447.
3. Rashad AM (2013) A comprehensive overview about the influence of different additives on the properties of alkali-activated slag—A guide for Civil Engineer. *Constr Build Mater* 47: 29–55.
4. Uzbaş B, Aydın AC (2019) Analysis of fly ash concrete with scanning electron microscopy and X-ray diffraction. *Adv Sci Technol Res J* 13: 100–110.
5. Yu J, Li G, Leung CKY (2018) Hydration and physical characteristics of ultrahigh-volume fly ash-cement systems with low water/binder ratio. *Constr Build Mate* 161: 509–518.
6. Feng J, Sun J, Yan P (2018) The influence of ground fly ash on cement hydration and mechanical property of mortar. *Adv Civ Eng* 2018: 4023178.
7. Saha AK (2018) Effect of class F fly ash on the durability properties of concrete. *Sustainable Environ Res* 28: 25–31.
8. Chindaprasirt P, Chotithanorm C, Cao HT, et al. (2007) Influence of fly ash fineness on the chloride penetration of concrete. *Constr Build Mater* 21: 356–361.
9. Singh GVPB, Subramaniam KVL (2016) Concrete using siliceous fly ash at very high levels of cement replacement: Influence of lime content and temperature. *2nd RN Raikar Memorial International Conference and Banthia-Basheer International Symposium on Advances in Science and Technology of Concrete*, Mumbai, India, 1–11.
10. Liu Z, Xu D, Zhang Y (2017) Experimental investigation and quantitative calculation of the degree of hydration and products in fly ash-cement mixtures. *Adv Mater Sci Eng* 2017: 2437270.
11. Atiş CD (2003) High-volume fly ash concrete with high strength and low drying shrinkage. J *Mater Civil Eng* 15: 153–156.
12. Plowman C, Cabrera JG (1996) The use of fly ash to improve the sulphate resistance of concrete. *Waste Manage* 16: 145–149.
13. Hemalatha T, Ramaswamy A (2017) A review on fly ash characteristics—Towards promoting high volume utilization in developing sustainable concrete. *J Cleaner Prod* 147: 546–559.
14. Hemalatha T, Mapa M, George N, et al. (2016) Physico-chemical and mechanical characterization of high volume fly ash incorporated and engineered cement system towards developing greener cement. *J Cleaner Prod* 125: 268–281.
15. Jung SH, Saraswathy V, Karthick S, et al. (2018) Microstructure characteristics of fly ash concrete with rice husk ash and lime stone powder. *Int J Concr Struct Mater* 12: 1–9.
16. Patil RA, Zodape SP (2011) X-ray diffraction and sem investigation of solidification/stabilization of nickel and chromium using fly ash. *E-J Chem* 8: S395–S403.
17. Pyatina T, Sugama T (2016) Acid resistance of calcium aluminate cement–fly ash F blends. *Adv Cem Res* 28: 433–457.
18. Wang A, Zhang C, Sun W (2003) Fly ash effects: I. The morphological effect of fly ash. *Cement Concrete Res* 33: 2023–2029.

19. Donatello S, Palomo A, Fernández-Jiménez A (2013) Durability of very high volume fly ash cement pastes and mortars in aggressive solutions. *Cem Concr Compos* 38: 12–20.
20. Garcia-Lodeiro I, Fernandez-Jimenez A, Palomo A (2013) Hydration kinetics in hybrid binders: Early reaction stages. *Cem Concr Compos* 39: 82–92.
21. Wang A, Zhang C, Sun W (2004) Fly ash effects: III. The microaggregate effect of fly ash. *Cement Concrete Res* 34: 2061–2066.
22. De Weerdt K, Haha MB, Le Saout G, et al. (2011) Hydration mechanisms of ternary Portland cements containing limestone powder and fly ash. *Cement Concrete Res* 41: 279–291.
23. Tang SW, Cai XH, He Z, et al. (2016) Hydration process of fly ash blended cement pastes by impedance measurement. *Constr Build Mater* 113: 939–950.
24. Kayali O (2004) Effect of high volume fly ash on mechanical properties of fiber reinforced concrete. *Mater Struct* 37: 318–327.
25. Siddique R (2004) Performance characteristics of high-volume Class F fly ash concrete. *Cement Concrete Res* 34: 487–493.
26. IS 516-1959 (reaffirmed 2004): Indian Standard Methods of Tests for Strength of Concrete. BIS, 1999. Available form: https://www.iitk.ac.in/ce/test/IS-codes/is.516.1959.pdf.
27. ASTM C1202-12, Standard Test Method for Electrical Indication of Concrete's Ability to Resist Chloride Ion Penetration. ASTM International, 2012. Available form https://www.astm.org/DATABASE.CART/HISTORICAL/C1202-12.htm.

AIMS Press